Journal Pre-proof

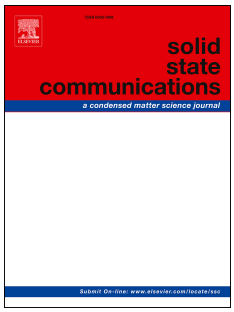

Magnetic properties of quasi-one-dimensional Ising-chain compounds $Fe_xCo_{1-x}Nb_2O_6$ at very low temperatures

P.W.C. Sarvezuk, C. Paulsen, J.B.M. da Cunha, M.A. Gusmão, O. Isnard

PII: S0038-1098(23)00271-5

DOI: https://doi.org/10.1016/j.ssc.2023.115334

Reference: SSC 115334

To appear in: *Solid State Communications*

Received Date: 5 June 2023

Revised Date: 23 August 2023

Accepted Date: 10 September 2023

Please cite this article as: P.W.C. Sarvezuk, C. Paulsen, J.B.M. da Cunha, M.A. Gusmão, O. Isnard, Magnetic properties of quasi-one-dimensional Ising-chain compounds $Fe_xCo_{1-x}Nb_2O_6$ at very low temperatures, *Solid State Communications* (2023), doi: https://doi.org/10.1016/j.ssc.2023.115334.

Magnetic properties of quasi-one-dimensional Ising-chain compounds $Fe_xCo_{1-x}Nb_2O_6$ at very low temperatures

PWC Sarvezuk[a,1], C Paulsen[b], JBM da Cunha[c], MA Gusmão[c], O Isnard[b]

[a]*Universidade Tecnológica Federal do Paraná, Campus Campo Mourão, Caixa Postal 271, 87301-899, Campo Mourão, Brazil*

[b]*Université Grenoble Alpes, Institut Néel, CNRS, BP166X, 38042 Grenoble Cédex 9, France*

[c]*Instituto de Física, Universidade Federal do Rio Grande do Sul, Caixa Postal 15051, 91501-970, Porto Alegre, Brazil*

Abstract

Combining very low-temperature experiments such as neutron diffraction, magnetometry, and specific-heat measurements, we report on the magnetic properties of the $Fe_xCo_{1-x}Nb_2O_6$ series of compounds. This investigation demonstrates that the ground state for x = 0.2, 0.4, and 0.6, previously reported as totally frustrated, is composed of Ising-like ferromagnetic chains that are antiferromagnetically ordered. Ordering at these compositions is observed to occur below 2 K. The magnetic structure is obtained from neutron diffraction, and susceptibility measurements allow us to estimate the values of intra- and interchain exchange constants, the former being clearly dominant. Fe/Co cation disorder reduces the average exchange strength within and between chains, reflecting the tendency to suppress long-range magnetic order. The diffuse magnetic signal observed by neutron diffraction slightly above the Néel temperature is analyzed to extract information on short-range magnetic correlations. Magnetization curves at 80 mK and specific-heat measurements reveal that an external magnetic field easily breaks the antiferromagnetic order, leading to a high magnetization due to the alignment of the ferromagnetic Ising chains.

Keywords: low-dimensional magnetism, neutron diffraction, magnetic specific heat, short-range order

[1] Corresponding author

Email address: pwcsarvezuk@gmail.com (PWC Sarvezuk)

1. Introduction

AB_2O_6 compounds (A = Fe, Co, Ni; B = Ta, Nb) have mainly been investigated for their interesting structural and magnetic properties. These compounds exhibit magnetic ordering at low temperatures (typically below 10 K), with a wide variety of magnetic phases, which can be classified as antiferromagnetic (AF), but differ from a simple Néel structure. One of the exciting characteristics of AB_2O_6 is low-dimensional magnetism. [1–12].

In particular, the tantalites ATa$_2$O$_6$ present weakly coupled magnetic planes [1, 13], whereas the niobates ANb$_2$O$_6$ exhibit quasi-one-dimensional magnetism [7, 14, 15]. This difference is associated with their distinct crystal-structure symmetries, respectively tetrahedral and rhombohedral. The columbite-structure niobates have also been investigated for their interesting optical and dielectric properties [16–20], with possible technological applications.

In the columbite (*Pbcn*) structure of ANb$_2$O$_6$, the A^{2+} and Nb^{5+} cations are located at the 4c and 8d positions, respectively, while the oxygen ions sit on three nonequivalent positions, forming octahedra surrounding the cations. These oxygen octahedra are distorted and alternatingly tilted along the c-axis (Fig. 1), forming zig-zag chains also characteristic of the α-PbO$_2$ structure [21, 22]. CoNb2O6 undergoes a transition from the paramagnetic phase to an ordered spin structure [14] at 2.95 K. Based on powder and single crystal neutron diffraction, Scharf *et al.* [23] investigated its magnetic phase diagram, later followed by Heid *et al.* [14, 24] and Kobayashi *et al.* [15, 17] with studies of magnetic properties. Later on, Sarvezuk *et al.* [25] reported neutron diffraction and susceptibility results confirming the presence of two magnetic transitions at 2.9 and 1.95 K. At an intermediate temperature of 2.5 K, a magnetic structure described by the propagation vector (0, 0.4, 0) was observed, whereas at 1.4 K two magnetic phases coexist, with propagation vectors (0,1/2,0) and (1/2,1/2,0), as revealed by neutron diffraction. Experimental observations of quantum criticality and exotic excitations in CoNb$_2$O$_6$ [26] triggered a renewed interest in this compound and its original magnetic properties [27–32].

FeNb$_2$O$_6$ was also found to show interesting magnetic properties. A collinear ordering with propagation vector (0,1/2,0) was first reported [33], and a noncollinear canted structure was deduced from magnetization measurements and group-theory analysis [34, 35]. Combining magnetic measurements and neutron diffraction, Heid and coworkers have observed a coexistence of phases with (0,1/2,0) and (1/2,1/2,0) propagation vectors in FeNb$_2$O$_6$ [7].

A detailed study of the Fe$_x$Co$_{1-x}$Nb$_2$O$_6$ series of compounds, for x = 0, 0.2, 0.4, 0.6, 0.8, and 1, was undertaken some time ago [36]. X-ray and neutron diffraction (ND) showed that the orthorhombic crystal structure is stable throughout the series. Furthermore, ND and magnetic measurements showed that magnetic order is preserved in the Fe-rich region (x = 0.8). In contrast, no long-range order was observed down to 2 K for x = 0.2, 0.4, and 0.6, despite the observation of short-range magnetic correlations. The low strength of magnetism in (Fe,Co)Nb$_2$O$_6$ compounds was interpreted as originating from cation disorder, which tends to randomize interchain interactions, thus favoring geometrical frustration due to the triangular arrangement of the chains concerning the transverse *ab* plane of the lattice (Fig. 1).

We revisit here the Fe$_x$Co$_{1-x}$Nb$_2$O$_6$ series, with a focus on the Fe concentrations x = 0.2, 0.4, and 0.6, which do not show magnetic ordering down to 2 K, performing a detailed investigation (on powder samples) of magnetic properties at very low temperatures. The present study aims to determine the intrinsic properties of the system in this composition range, particularly whether only short-range correlations exist due to frustration or a long-range magnetic order develops below 2K. Our results confirm the latter scenario. We found that magnetic transitions occur at or slightly below 2 K, although well-developed magnetic moments are only observable at still lower temperatures.

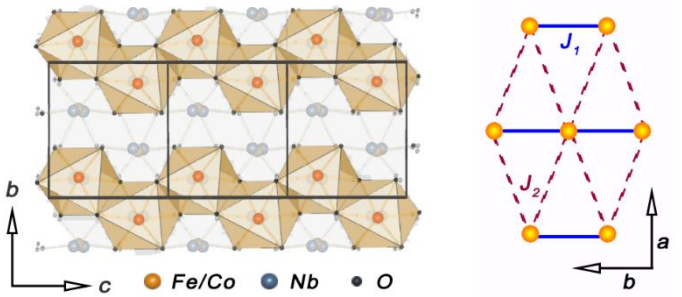

Figure 1: (Color online) Left: a sketch of the Fe$_x$Co$_{1-x}$Nb$_2$O$_6$ crystal structure in the *bc* plane showing the zig-zag chains of (Fe,Co) cations running along the c axis; black lines show the unit cell. Right: schematic representation of the magnetic exchange interactions between zig-zag cation chains. Different interchain exchange constants, J_1 and J_2, are indicated. Their average value is referred to as $J_\perp$ in Sec. 3.4.

The following section describes the experimental conditions and techniques employed, after which we present and discuss our results. Magnetic measurements are discussed in Sec. 3.1, specific-heat measurements at very low temperatures are shown in Sec. 3.2, the neutron-diffraction investigation is presented in Sec. 3.3, and a model evaluation of exchange constants is discussed in Sec. 3.4. Finally, Sec. 4 contains a summary of our results and conclusions.

2. Experimental

Powder samples of $FeNb_2O_6$ and $CoNb_2O_6$ were prepared as described in Ref. [36]. Magnetic measurements were undertaken on these samples in a wide temperature range – from 1.7 K to 300 K, using the extraction method with an experimental setup described elsewhere [37]. Both isothermal magnetization, $M(H)$, and susceptibility as a function of temperature, $\chi(T)$, were measured. For the latter, a magnetic field $\mu_0 H$ = 0.5 T was employed. At the same time, $M(H)$ curves were recorded for magnetic fields in the range $\mu_0 H$ = 0–10 T. Additionally, magnetization and susceptibility measurements were made at very low temperatures, down to approximately 80 mK. Two SQUID-based magnetometers were used, designed, and built at the Néel Institute (Grenoble, France). One is dedicated to studies in high fields (up to 8 T). The other has higher sensitivity for low-field measurements. Both are equipped with miniature ^{3}He/^{4}He dilution refrigerators. Moreover, data can be obtained by the extraction method, allowing us to measure the absolute values of the magnetization.

Specific heat was measured by the pulsed relaxation method, down to 0.3 K and in the field range from 0 to 5 T, using a dedicated ^{3}He insert implemented in a commercial setup (Quantum Design PPMS).

Neutron-diffraction patterns were recorded on the D1B powder diffractometer operated by the CNRS at the Institut Laue Langevin (ILL) in Grenoble, France. A wavelength of 2.52 Å was used, with 400 cells multidetector covering an angular 2θ range of 5° to 85°, with a scan step of 0.2°. Diffractograms from room temperature down to 1.8 K used a standard orange cryostat, the powder sample being mounted in a cylindrical vanadium sample holder. For measurements at lower temperatures, a ^{3}He refrigerator was employed, enabling to carry out of experiments from 20 K down to 0.4 K. Crystallographic and magnetic parameters were refined using the FullProf program [38].

3. Results and discussion

We will mainly focus on results for the compositions with Fe content x = 0.2, 0.4, and 0.6, which do not show magnetic order above 2 K [36].

3.1. Magnetization measurements

Magnetization isotherms recorded at 80 mK are plotted in Fig. 2 for x = 0.2, 0.4, and 0.6. One can see that they resemble large-moment paramagnetic curves. A noticeable feature in Fig. 2 is the incomplete saturation of the magnetization even at fields as high as $\mu_0 H$ = 8 T. This should be expected, as we are dealing with strong spin anisotropy and polycrystalline samples so that only the regions where the easy axis is nearly aligned with the applied field will substantially contribute to the overall magnetization. It is worth remarking that the high-field magnetization is most significant for x = 0.6, and decreases as the Fe content is reduced, which can be attributed to the larger moment of Fe^{2+} (S = 2) in comparison to Co^{2+} (S = 3/2), both in high-spin configuration.

3.2. Specific-heat measurements at low temperature

Specific-heat data collected in the low-temperature range, down to 300 mK, are plotted for the x = 0.2 sample in Fig. 3, both at zero magnetic fields and for three different intensities of the applied field. Similar curves are obtained for x = 0.4 and 0.6. It is interesting to notice that increasing the magnetic field shifts the broad bump of magnetic origin towards higher temperatures and significantly increases the specific-heat values above the bump.

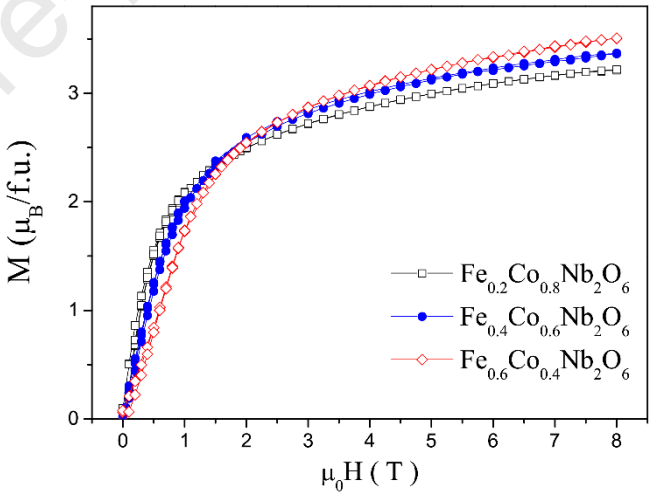

Figure 2: Comparison of the magnetization curves recorded at 80 mK for the $Fe_xCo_{1-x}Nb_2O_6$ compounds with x=0.2, 0.4, and 0.6.

The overall behavior of the curves in Fig. 3 can be qualitatively reproduced by the exact specific heat of independent ferromagnetic Ising chains (adding a smooth power-law term to account for the lattice contribution). This agrees with a weak inter-chain coupling deduced from the magnetic measurements (Sec. 3.1).

3.3. Neutron diffraction

Rietveld refinement of our neutron-diffraction data, including experiments at very low temperatures, indicates that the orthorhombic structure of the $Fe_xCo_{1-x}Nb_2O_6$ samples is preserved down to 0.4 K. The unit cell

parameters, the positional parameters, and the R factors of the Rietveld refinements are listed in Table 1.

Table 1: Structural parameters derived from refinements of the neutron diffraction patterns recorded at 2 K for $Fe_xCo_{1-x}Nb_2O_6$ powder samples (x = 0.2, 0.4, 0.6). The site occupancies for the Nb and O atoms were fixed at 100%. The atomic displacement parameters were not refined, and a fixed value of 0.05 Å^2 was used.

Atom		x = 0.2	0.4	0.6
Fe/Co	x	0	0	0
	y	0.163(4)	0.1161(4)	0.1255(4)
	z	0.25	0.25	0.25
Nb	x	0.1481(5)	0.1623(5)	0.1634(5)
	y	0.4550(12)	0.3053(12)	0.3165(11)
	z	0.8047(4)	0.7394(3)	0.7337(3)
O1	x	0.0524(3)	0.0967(3)	0.0889(3)
	y	0.3046(5)	0.3539(8)	0.3581(9)
	z	0.5363(3)	0.4261(11)	0.3822(12)
O2	x	0.0946(3)	0.0838(2)	0.0889(3)
	y	0.1196(9)	0.1453(9)	0.1397(9)
	z	0.9774(1)	0.9256(11)	0.9517(11)
O3	x	0.2156(5)	0.2574(4)	0.2619(6)
	y	0.1937(8)	0.0734(9)	0.0089(9)
	z	0.6571(13)	0.5353(11)	0.5718(1)
a (Å)		14.1007(2)	14.1590(12)	14.1842(4)
b (Å)		5.6630(2)	5.7121(2)	5.7123(3)
c (Å)		5.0507(1)	5.0359(1)	5.0288(1)
Volume (Å^3)		403.3(1)	407.2(2)	407.5(2)
Occ (%)	Fe	17(1)	44(1)	58(1)
	Co	83(1)	56(1)	42(1)
R_{wp} (%)		7.8	5.5	5.1
R_B (%)		8.3	6.3	7.0

3.3.1. *Short-range order at low temperature*

In our previous investigation [36], carried out at around 2 K or higher temperatures, no Bragg peaks characteristic of long-range magnetic order were observed for x = 0.2, 0.4, and 0.6. However, a careful look at the difference plot between patterns recorded at 20 K (in the paramagnetic state) and 1.8 K revealed a broad signal around 2θ = 11.5°. Although this can be attributed to short-range magnetic correlations, their origin was unclear since they could indicate an approach to an ordered state setting in at still lower temperatures. Still, it could also be due to the suppression of long-range order by frustration of the exchange interactions.

The short-range order (SRO) bump observed at 1.8 K is centered at a wavevector of module $q \simeq 0.5$ Å^{-1}, and its half-width is much larger than the experimental resolution. To extract information from this SRO diffuse signal, we fit the experimental data considering a description of the magnetic scattering due to short-range spin-spin correlations.

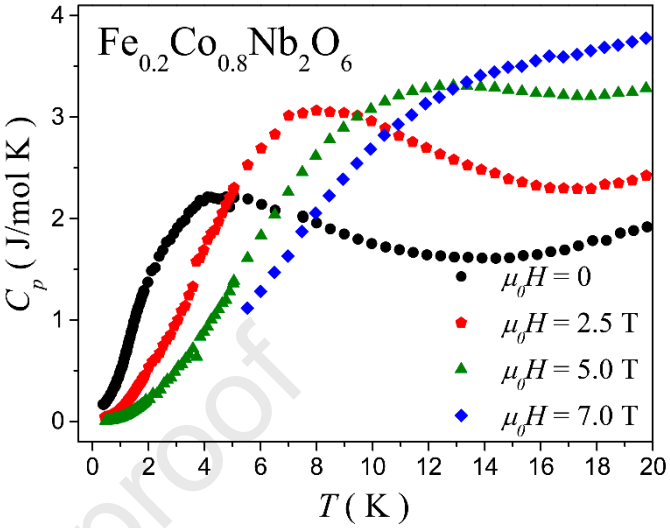

Figure 3: Typical Low-temperature behavior of the specific heat of $Fe_xCo_{1-x}Nb_2O_6$ samples, here shown for x = 0.2 and a few different applied magnetic fields.

In this framework, the signal intensity is described [39–42] by an expression of the type

$$I(q) = \sum_{i=1}^{n} c_i \Gamma_i \frac{\sin qR_i}{qR_i} + B \qquad (1)$$

Where the summation is over coordination shells of radii R_i surrounding a reference atom, c_i is the number of magnetic ions in the i-th shell, the coefficients Γ_i is proportional to the average spin correlations at each distance, and B is a background-correcting constant.

We restrict summation to distances up to 10 Å for the present calculation. We use data obtained by subtracting the paramagnetic-state signal at 20 K from that recorded at 1.8 K, with Γ_i and B as adjustable parameters. An example fitting is given in Fig. 4. Similar fittings for all the studied compositions allowed us to obtain relative spin-spin correlations averaged over each coordination shell, summarized in Table 2. It is seen that ferromagnetic correlations exist within the zigzag chains, that is, between cations at about 3.0 and 4.97 Å from the reference one (nearest neighbors and next-nearest neighbors, respectively). The correlations between magnetic cations of different chains, corresponding to the shortest interchain distances 5.03, 5.7, and 7.6 Å, are found to be antiferromagnetic for all compositions. These results are

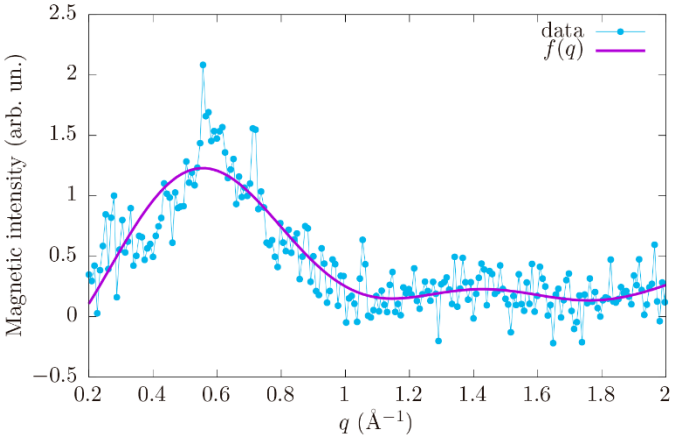

Figure 4: Fitting of the diffuse magnetic signal (points) obtained from the difference between neutron-diffraction patterns recorded at 20 K and 2K (close to the Néel temperature) for $Fe_{0.6}Co_{0.4}Nb_2O_6$ using Eq.1.

Table 2: Composition dependence of magnetic correlations for increasing atomic distances in the lattice, as derived from fittings of the low-temperature neutron diffuse scattering signal of magnetic origin. The values are normalized to nearest-neighbor correlations.

Fe fraction	Relative spin-spin correlation				
0.2	1	-0.51	0.79	-0.59	-0.10
0.4	1	-0.60	0.93	-0.69	-0.12
0.6	1	-0.65	0.83	-0.51	-0.16
Typical distance (Å)	3.0	5.03	4.97	5.7	7.6

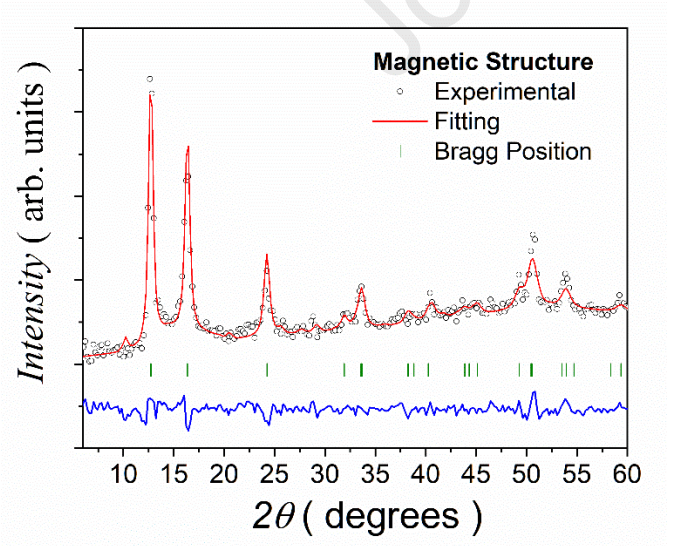

Figure 5: Refinement of the neutron diffraction pattern of $Fe_{0.6}Co_{0.4}Nb_2O_6$ recorded at 400 mK after the nuclear contribution from the paramagnetic state was subtracted.

In good agreement with the magnetic structure observed at very low temperatures, as will be discussed next, the observed SRO is a precursor to a truly ordered state.

3.3.2. Neutron diffraction down to 400 mK

To check for possible magnetic ordering of the $Fe_xCo_{1-x}Nb_2O_6$ compounds at very low temperatures, we recorded neutron powder-diffraction patterns down to 400 mK. The obtained results are exemplified in Fig. 5 for the x = 0.6 composition. It is clear that Bragg reflections appear upon cooling, thus ruling out the hypothesis of complete frustration with the magnetic interactions for this compound. Similar conclusions are reached for the other two compositions, x = 0.2 and 0.4.

Analysis of the diffraction patterns recorded between 0.4 and 1.6 K indicate that the magnetic reflections can be indexed with the propagation vector (0,1/2,0) in this temperature range. A summary of the Rietveld refinement results is given in Table 3. The thermal evolution of the different patterns is shown in Fig. 6, corresponding to decreasing magnetic moments with temperature, as listed in Table 4. The most considerable magnetic moment, obtained for x = 0.6 at 0.4 K, was 2.57 μ_B per magnetic cation, falling to about 60% of this value at 1.6 K. As a general trend, the refined magnetic moments approach saturation below 0.8 K and are no longer observable at 2 K.

Table 3: Structural parameters derived from Rietveld refinement of the neutron-diffraction pattern recorded at 400 mK for $Fe_{0.2}Co_{0.8}Nb_2O_6$ powder sample using (0,1/2,0) as propagation vector. The average Fe/Co magnetic moment was determined to be 2.57μ_B, and the fitting control parameters were R_{wp} = 4.5%, R_B = 3.3%, and R_B^{Mag} = 26.7%.

a (Å)		b (Å)	c (Å)
14.082(3)		5.684(4)	5.009(5)
Atom	x	y	z
Fe/Co	0	0.1450(4)	0.25
Nb	0.1633(2)	0.3581(2)	0.7337(4)
O1	0.0889(2)	0.3725(3)	0.3833(3)
O2	0.0852(3)	0.1397(5)	0.9517(1)
O3	0.2620(0)	0.0889(1)	0.5718(2)

Table 4: Magnetic moments obtained from Rietveld refinement of the neutron-diffraction patterns of $Fe_xCo_{1-x}Nb_2O_6$ compounds (x = 0.20, 0.4, 0.6), recorded at the indicated temperatures.

Sample	Fe/Co moments (μ_B)				
$Fe_{0.2}Co_{0.8}Nb_2O_6$	2.28	2.34	2.35	2.08	1.43
$Fe_{0.4}Co_{0.6}Nb_2O_6$	1.77	1.84	1.69	1.42	1.15
$Fe_{0.6}Co_{0.4}Nb_2O_6$	2.57	2.47	2.26	1.96	1.48
Temperature (K)	0.4	0.70	1.00	1.30	1.60

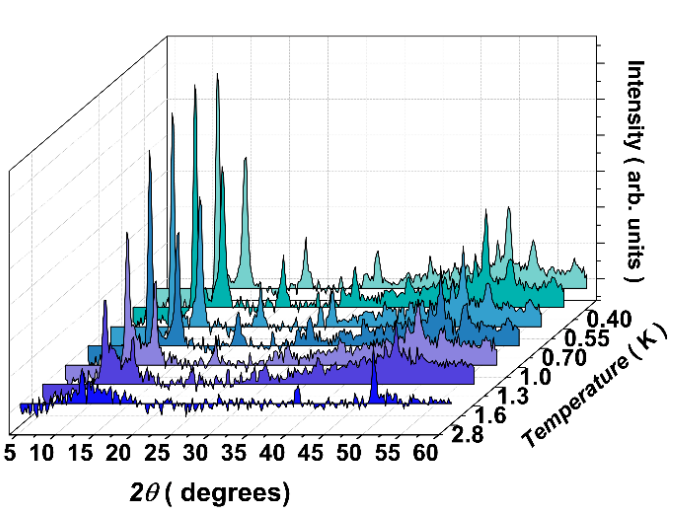

Figure 6: Temperature dependence of the magnetic part of neutron diffraction patterns recorded at the indicated temperatures for $Fe_{0.6}Co_{0.4}Nb_2O_6$.

3.4. Determination of the exchange constants

Ordering temperatures of the $Fe_xCo_{1-x}Nb_2O_6$ compounds with x = 0.20, 0.4, and 0.6 were estimated from the thermal variation of the neutron diffraction pattern. They appear in Table 5, together with T_N values for the other samples (x = 1.0, 0.2, and 0.0) and values of the Curie-Weiss temperature θ_W for the whole series, already reported in Ref. [36]. As can be seen, T_N is substantially smaller than θ_W, indicating the presence of significant frustration in the system. This can be understood considering the existence of a triangular network of Ising chains in this structure, as shown in Fig. 1. The frustration ratio θ_W/T_N is close to 1.3 at both pure limits but grows to about 2.3 for x = 0.2 and 0.4.

It has been demonstrated elsewhere [36] that, in the scenario of weakly interacting Ising chains, the intrachain J_0, and interchain $J_\perp$ exchange interactions can be derived from known (measured) values of T_N and θ_W through the relations

$$\theta_W = (2J_0 + z_\perp J_\perp)S^2 \qquad (2)$$

$$z_\perp^* |J_\perp| S^2 = T_N e^{2S^2 J_0/T_N} \qquad (3)$$

Where S represents the average spin of the cations and $z_\perp^*$ is an adequate number of nearest-neighbor chains, we use $z_\perp^*$= 2 because four of the six interchain interactions tend to cancel each other in the observed ordered phases (see Fig. 1).

The exchange constants obtained here for x = 0.20, 0.4, and 0.6 are listed in Table 5, which also includes, for comparison, the values previously reported [36] for x = 0, 0.8, and 1. It is worth remarking that the intrachain exchange constant J_0 is at least one order of magnitude larger than the average interchain coupling $J_\perp$. This reflects the relatively strong ferromagnetic coupling between cations within the Ising zig-zag chains. The values of $J_\perp$ are much smaller (by a factor of 2 to 5) for the intermediate concentrations compared with the end members of the series, x = 0 and 1. These remarkably weak values of $J_\perp$ undoubtedly contribute to the observed lowering of the ordering temperature for x = 0.20, 0.4, and 0.6, also confirming the scenario of weakly interacting Ising chains.

4. Conclusions

Unlike the $(Ni,Fe)Nb_2O_6$ system [42], which does not order down to 400 mK for x = 0.2, 0.4, 0.6, 0.8, we demonstrate here that the $Fe_xCo_{1-x}Nb_2O_6$ series of compounds do order below or near 2 K. According to neutron diffraction experiments, these compounds exhibit long-range magnetic order at very low temperature, but only short-range correlations are observed around 2 K. The diffuse magnetic scattering has been fitted to estimate relative values of spin-spin correlations. This measurement led us to conclude that interchain correlations are dominantly antiferromagnetic, while stronger positive spin-spin correlations exist within the zig-zag cation chains, indicating antiferromagnetic intrachain exchange. Thermal dependence of Fe/Co magnetic moments has been determined down to 400mK. The largest value is obtained for x = 0.6, with an average magnetic moment of 2.57 μ_B per Fe/Co cation.

Table 5: Néel temperature, Curie-Weiss temperature, and paramagnetic parameters of the $Fe_xCo_{1-x}Nb_2O_6$ series of compounds, the intra Ising chain J_0 and the inter Ising chain exchange constants derived from the above values are also listed for all the studied compositions.

Sample	T_N (K)	θ_W (K)	J_0 (K)	$J_\perp$ (K)
1	4.9	6.6	1.12	-0.098
0.80	2.4	3.3	0.61	-0.052
0.60	2.0	3.4	0.64	-0.039
0.40	1.9	4.2	0.81	-0.02
0.20	1.8	4.2	0.90	-0.027
0	2.9	3.9	1.18	-0.104

The antiferromagnetic coupling between chains and their triangular topological arrangement are common ingredients of a frustrated system. This frustration is probably enhanced by cation disorder due to substitutions, which tend to average the different intrachain couplings J_1 and J_2 (see Fig. 1) to a single effective $J_\perp$. This is most probably at the origin of the very low ordering temperatures observed in the $Fe_xCo_{1-x}Nb_2O_6$ series of compounds. In the weakly

interacting Ising chains hypothesis, we added a mean-field treatment of the interchain coupling to accurately describe isolated ferromagnetic Ising chains. This allowed the determination of both exchange constants from experimental values of transition temperatures and magnetic susceptibilities. The calculated intrachain interaction is about one order of magnitude larger than the interchain one, in agreement with the starting assumption. Further confirmation of this scenario of weakly interacting Ising chains comes from magnetization curves at 80 K as well as specific-heat measurements, both revealing that the antiferromagnetic order is easily broken by an applied magnetic field, leading to a ferromagnetic alignment of the chains.

Interesting possible developments of the work reported here could include a study of magnetic excitations in the $Fe_xCo_{1-x}Nb_2O_6$ series. In particular, this would permit exploring the complex phase diagram for varying temperatures and magnetic field that has been theoretically predicted by Lee et al. [27] for the reference compound $CoNb_2O_6$. Furthermore, experimental investigations in single crystals would allow us to analyze the quantum behavior of a transverse field Ising system [26–28], including the presence of disorder and frustration effects.

Acknowledgments

This work was supported in part by the French-Brazilian cooperation program CAPES-COFECUB No. Ph 937/19, and by the Brazilian agency Conselho Nacional de Desenvolvimento Científico e Tecnológico (CNPq). The authors would like to thank the sample-environment (SANE) staff of the Institut Laue Langevin (CNRS, Grenoble, France) for its efficiency in setting up the low-temperature equipment. O. I., on behalf of the Université Grenoble Alpes (Grenoble, France), is thankful to the Region Rhône Alpes, France, for invaluable support through the ARCUS-Brésil program.

References

[1] S. M. Eicher, J. E. Greedan, K. J. Lushington, J. Sol. State Chem. 62 (1986) 220.

[2] Y. Muraoka, T. Idogaki, N. Uryu, J. Phys. Soc. Jpn. 57 (1988) 1758.

[3] E. M. L. Chung, M. R. Lees, G. J. McIntyre, C. Wilkinson, G. Balakrishnan, J. P. Hague, D. Visser, D. M. Paul, J. Phys.: Conden. Matter 16 (2004) 7837.

[4] R. K. Kremer, J. E. Greedan, E. Gmelin, W. Dai, M. A. White, S. M. Eicher, K. J. Lushington, J. Phys. Colloques 49 (C8) (1988) C8–1495.

[5] J. P. Hague, E. M. L. Chung, D. Visser, G. Balakrishnan, E. Clementyev, D. M. Paul, M. R. Lees, J. Phys.: Condens. Matter 17 (2005) 7227.

[6] J. Reimers, J. E. Greedan, C. V. Stager, K. R., J. Solid State Chem. 83 (1989) 20.

[7] C. Heid, H. Weitzel, F. Bourdarot, R. Calemczuk, T. Vogt, H. Fuess, J. Phys. Condens. Matter 8 (1996) 10609.

[8] H. Ehrenberg, G. Wltschek, J. Rodriguez-Carvajal, T. Vogt, J. Magn. Magn. Mater. 184 (1988) 111.

[9] E. J. Kinast, V. Antonietti, D. Schmitt, O. Isnard, J. B. M. da Cunha, M. A. Gusmão, C. A. dos Santos, Bicriticality in $Fe_xCo_{1-x}Ta_2O_6$, Phys. Rev. Lett. 91 (19) (2003) 197208.

[10] R. K. Kremer, J. E. Greedan, J. Sol. St. Chem. 73 (1988) 579.

[11] S. R. de Oliveira Neto, E. J. Kinast, M. A. Gusmão, C. A. dos Santos, O. Isnard, J. B. M. da Cunha, J. Phys.: Condens. Matter 19 (2007) 356210.

[12] S. R. Oliveira Neto, E. J. Kinast, O. Isnard, J. B. M. da Cunha, M. A. Gusmão, C. A. dos Santos, J. Magn. Magn. Mater. 320 (2008) e125.

[13] L. I. Zawislak, G. L. F. Fraga, da Cunha J. B. M., D. Schimitt, A. S. Carriço, C. A. dos Santos, J. Phys. Condens. Matter 9 (1997) 2295.

[14] C. Heid, H. Weitzel, P. Burlet, M. Bonnet, W. Gonschorek, T. Vogt, J. Norwig, H. Fuess, J. Magn. Magn. Mater 151 (1995) 123.

[15] S. Kobayashi, S. Mitsuda, K. Prokes, Phys. Rev. B 63 (2000) 24415.

[16] Y. Zhou, Z. Lu, M. Qiu, A. Zhang, Q. Ma, H. Zhang, Z. Yang, Materials Science and Engineering B 140 (2007) 128.

[17] S. Kobayashi, S. Mitsuda, M. Ishikawa, K. Miyatani, K. Kohn, Phys. Rev. B 60 (1999) 3331.

[18] A. M. J. Ye Z. Zhou, Int. J. Hydrogen Energy 63 (2003) 24415.

[19] R. C. Pullar, N. M. A. C. Vaughan, J. Phys. D: Appl. Phys. 37 (2004) 348.

[20] R. C. Pullar, J. Am. Ceram. Soc. 92 (2009) 563.

[21] R. W. G. Wyckoff, Crystal Structure, Wiley, New York, 1965.

[22] A. I. Zaslavsky, Y. D. Kondrashev, S. S. Tolkachev, Dokl. Akad. Nauk (SSSR) 75 (1950) 559.

[23] W. Scharf, H. Weitzel, I. Yaeger, I. Maartense, B. M. Wanklyn, J. Magn. Magn. Mater. 13 (1979) 121.

[24] C. Heid, H. Weitzel, P. Burlet, M. Winkelmann, H. Ehrenberg, H. Fuess, Physica B: Condensed Matter 234-236 (1997) 574–575.

[25] P. W. C. Sarvezuk, E. J. Kinast, C. V. Colin, M. A. Gusmão, J. B. M. da Cunha, O. Isnard, J. Appl. Phys. 109 (2011) 07E160.

[26] R. Coldea, D. A. Tennant, E. M. Wheeler, E. Wawrzynska, D. Prabhakaran, M. Telling, K. Habicht, P. Smeibidl, K. Kiefer, Science 327 (2010) 177.

[27] S. Lee, R. K. Kaul, L. Balents, Nat. Phys. 6 (2010) 702.

[28] C. M. Morris, R. Vald´es Aguilar, A. Ghosh, S. M. Koohpayeh, J. Krizan, R. J. Cava, O. Tchernyshyov, T. M. McQueen, N. P. Armitage, Phys. Rev. Lett. 112 (2014) 137403.

[29] N. J. Robinson, F. H. L. Essler, I. Cabrera, R. Coldea, Phys. Rev. B 90 (2014) 174406.

[30] S. Kobayashi, S. Hosaka, H. Tamatsukuri, T. Nakajima, S. Mitsuda, K. Prokes, K. Kiefer, Phys. Rev. B 90 (2014) 060412.

[31] I. Cabrera, J. D. Thompson, R. Coldea, D. Prabhakaran, R. I. Bewley, T. Guidi, J. A. Rodriguez-Rivera, C. Stock, Phys. Rev. B 90 (2014) 014418.

[32] A. W. Kinross, M. Fu, T. J. Munsie, H. A. Dabkowska, G. M. Luke, S. Sachdev, T. Imai, Phys. Rev. X 4 (2014) 031008.

[33] H. Weitzel, Anorg. Allg. Chem. 380 (1971) 119.

[34] I. Yaeger, A. H. Morrish, B. M. Wanklyn, Phys. Rev. B 15 (1977) 1465.

[35] I. Yaeger, A. H. Morrish, B. M. Wanklyn, B. J. Garrard, Phys. Rev. B 16 (1977) 2289.

[36] P. W. C. Sarvezuk, E. J. Kinast, C. V. Colin, M. A. Gusmão, J. B. M. da Cunha, O. Isnard, Phys. Rev. B 83 (17) (2011) 174412.

[37] A. Barlet, J. C. Genna, P. Lethuillier, Cryogenic 31 (1991) 801.

[38] J. Rodriguez-Carvajal, Physica B 192 (1993) 55.

[39] E. F. Bertaut, P. Burlet, Solid State Commun. 5 (1967) 279.

[40] A. Wiedenmann, P. Burlet, H. Scheuer, P. Convert, Solid State Commun. 38 (1981) 129.

[41] I. Mirebeau, A. Apetrei, J. Rodríguez-Carvajal, P. Bonville, A. Forget, D. Colson, V. Glazkov, J. P. Sanchez, O. Isnard, E. Suard, Phys. Rev. Lett. 94 (2005) 246402.

[42] P. W. C. Sarvezuk, M. A. Gusmão, J. B. M. da Cunha, O. Isnard, Phys. Rev. B 86 (2012) 054435.

Highlights

- **Exploring AB_2O_6 Compounds:** Investigating the structural and magnetic properties of AB_2O_6 compounds (A = Fe, Co, Ni; B = Ta, Nb) with magnetic ordering at low temperatures and diverse magnetic phases.
- **Unveiling Low-Dimensional Magnetism:** AB_2O_6 compounds reveal intriguing low-dimensional magnetism, driven by distinct crystal structure symmetries of niobates.
- **Crystal Structure Insights:** ANb_2O_6's columbite structure showcases alternatingly tilted oxygen octahedra, forming distinctive zig-zag chains within the lattice.
- **Probing $CoNb_2O_6$ and $FeNb_2O_6$ transitions and magnetic characteristics:** Investigating $CoNb_2O_6$'s transition from paramagnetic to ordered spin structure at 2.95 K using a combination of neutron diffraction and magnetic measurements. Understanding the magnetic properties of $FeNb_2O_6$, highlighting collinear and noncollinear magnetic ordering phases, including the coexistence of different magnetic structures.
- **Detailed $Fe_xCo_{1-x}Nb_2O_6$ Study:** In-depth analysis of $Fe_xCo_{1-x}Nb_2O_6$ compounds at varying Fe concentrations (x = 0.2, 0.4, 0.6) revealing magnetic ordering phenomena below 2 K.
- **Deciphering Short-Range Order:** Identifying short-range magnetic correlations through neutron diffraction signals provides insights into the precursor states leading to ordered magnetic arrangements.
- **Unraveling Exchange Constants:** Determination of intrachain and interchain exchange constants, emphasizing the dominance of intrachain interactions due to ferromagnetic coupling within zig-zag chains.

Author Statement

We sincerely thank the distinguished reviewers for carefully evaluating our manuscript. We appreciate their confidence in our research's quality and recognition of its contribution to solid-state communications. Their insightful comments and suggestions have undoubtedly contributed to improving our work investigating magnetic properties in the $Fe_xCo_{1-x}Nb_2O_6$ series of compounds. We appreciate the rigorous examination of our research, which has allowed us to present a more comprehensive and accurate study.

Their constructive comments have undoubtedly enriched our study and improved the clarity and presentation of our findings. We have taken their suggestions seriously and made the necessary revisions to address their raised points.

Both reviewers' attention to detail and expertise have significantly enriched our work. Their contributions have led to a more rigorous and comprehensive presentation of our research findings. We are confident that the combination of their insights has strengthened the quality and impact of our manuscript.

Once again, we express our deep gratitude to the reviewers for their time, effort, and valuable insights. Their contributions have been instrumental in improving our manuscript and advancing the knowledge in our field.

Sincerely,

Paulo Sarvezuk, Corresponding Author.

Professor UTFPR – pwcsarvezuk@gmail.com

Declaration of interests

☒ The authors declare that they have no known competing financial interests or personal relationships that could have appeared to influence the work reported in this paper.

☐ The authors declare the following financial interests/personal relationships which may be considered as potential competing interests: